

Research Article

Performance and Characterization for Blend Membrane of PES with Manganese(III) Acetylacetonate as Metalorganic Nanoparticles

H. Abdallah,¹ M. S. Shalaby,¹ and A. M. H. Shaban²

¹Chemical Engineering and Pilot Plant Department, Engineering Research Division, National Research Centre, 33 El Bohouth Street (Former El Tahrir Street), P.O. Box 12622, Dokki, Giza, Egypt

²Water Pollution Research Department, National Research Centre, 33 El Bohouth Street (Former El Tahrir Street), P.O. Box 12622, Dokki, Giza, Egypt

Correspondence should be addressed to H. Abdallah; drhebaabdallah3@gmail.com

Received 8 July 2015; Revised 23 August 2015; Accepted 2 September 2015

Academic Editor: Sébastien Déon

Copyright © 2015 H. Abdallah et al. This is an open access article distributed under the Creative Commons Attribution License, which permits unrestricted use, distribution, and reproduction in any medium, provided the original work is properly cited.

This study describes the preparation, characterization, and evaluation of performance of blend Polyethersulfone (PES) with manganese(III) acetylacetonate $Mn(acac)^3$ to produce reverse osmosis blend membrane. The manganese(III) acetylacetonate nanoparticles were prepared by a simple and environmentally benign route based on hydrolysis of $KMnO_4$ followed by reaction with acetylacetone in rapid stirring rate. The prepared nanoparticle powder was dissolved in polymer solution mixture to produce RO PES/ $Mn(acac)^3$ blend membrane, without any treatment of Polyethersulfone membrane surface. The membrane morphology, mechanical properties, and performance were presented. The scanning electron microscopy (SEM) images have displayed a typical asymmetric membrane structure with a dense top layer due to the migration of $Mn(acac)^3$ nanoparticles to membrane surface during the phase inversion process. Contact angle measurements have indicated that the hydrophilicity of the membrane was improved by adding $Mn(acac)^3$. AFM images have proved excellent pores size distribution of blend membrane and lower surface roughness compared with bare PES. The desalination test was applied to blend membrane, where the blend membrane provided good performance; particularly, permeate flux was $24.2 \text{ Kg/m}^2\cdot\text{h}$ and salt rejection was 99.5%.

1. Introduction

Most polymeric membranes are often prepared from the same materials, but under various membrane formation conditions, according to the required membrane type [1–3]. The polymeric materials such as poly(vinylidene fluoride), Polysulfone, Polyethersulfone, poly(acrylonitrile), and poly(vinyl chloride) copolymers are used to produce UF and MF membranes. RO and NF membranes are made of cellulose acetate, tricellulose acetate, Polyethersulfone, or Polysulfone coated with aromatic polyamides. Recently, the production of cheap antifouling RO membranes is required to serve the global demands for water desalination [1–3]. Blending of polymers with nanomaterials is a modern technological way for providing excellent polymeric membranes

with set of desired properties at the lowest cost such as a combination of strength and toughness, impact strength or solvent resistance, and good performance [3–5]. The most common methods to functionalize the nanomaterials on the membrane surface are expressed as follows: vapor deposition, electrophoretic coating, and dip coating, based on deposition of nanomaterials on the membrane surface. The blending method depends on the introduction of the nanomaterials on the backbone of the polymeric membrane; therefore the stability of the nanomaterials on the blending membranes has been achieved compared with precipitation methods [2–12].

Phase separation in polymer solutions is one of the most important and popular techniques for fabricating different functional polymeric materials that are widely used in engineering applications [5–8]. Using a phase separation process

in the fabrication of nanomaterials blending membranes leads to the formation of a top selective layer from nanomaterials connected to the membrane backbone [2–8].

Blending of inorganic nanoparticles such as TiO_2 , Al_2O_3 , SiO_2 , and Fe_3O_4 with a polymer solution during membrane preparation could improve the antifouling properties of the membranes [2–8].

Metal acetylacetonate complexes are widely used in various chemical reactions as catalyst and cocatalysts such as oligomerization, polymerization, isomerization, and hydrogenation [9–13]. The unique attributes of these coordination complexes are the tris-chelate complexes which occur due to the cardinal difference in two possible ligand bonding processes. The metal acetylacetonates such as $\text{Cr}(\text{acac})^3$, $\text{Al}(\text{acac})^3$, $\text{V}(\text{acac})^3$, $\text{Pt}(\text{acac})^2$, $\text{Cu}(\text{acac})^3$, $\text{Co}(\text{acac})^2$, $\text{Fe}(\text{acac})^3$, and $\text{Mn}(\text{acac})^3$ have high dispersion degree of supported metal acetylacetonates achievable due to their H-bonding with surface groups of support or ligand substitution [9–13]. However, these compounds could be used in polymeric coatings as a stabilizer of cross-linking reaction [9, 13], catalyst of the drying process [12, 14], and toughening agent [10]. Metalorganic compound are compounds consisting of metal ions or clusters coordinated to organic molecules to form one-, two-, or three-dimensional structures which are porous. The merits of these materials are huge surface area and pores volume leads them to be useful for separation applications [15].

Using metal acetylacetonate complex nanomaterials as metalorganic compound, in a membrane preparation could lead to improving the membrane performance due to high selectivity and permeability. In addition, the hydrophilicity, strength, stiffness, water permeability, and antifouling properties of the membrane could be enhanced by introducing metalorganic nanomaterials into membrane matrix [15–21].

Polyethersulfone (PES) is a famous polymer used in a membrane preparation. The advantages of Polyethersulfone membrane are high performance engineering thermoplastic, good mechanical properties, high glass transition temperature, and excellent thermal and chemical stability [22]. Polyethersulfone is usually used to prepare UF membranes, but the RO Polyethersulfone surface must be treated by interfacial polymerization process to be used in the desalination process [23]. Interfacial polymerization is the main process of Polyethersulfone membrane surface treatment, where thin film layer will be precipitated on the surface, forming dense skin selective layer, but this process needs hazard and expensive chemicals [23–25]. Accordingly, the introduction of various types of nanoparticles in membrane structure could provide nanofiltration and reverse osmosis membrane without any further treatment [2–8].

The novelty of this work is to benefit from the new complex nanomaterial compounds that have properties that combine organic and inorganic compounds and can access the polymeric membrane by H-bonding to the membrane surface or in the backbone of the membrane. Thus, the control of membrane pore size and hydrophilicity will be improved.

In this study, the preparation of blend membrane Polyethersulfone (PES) with metalorganic nanoparticle manganese(III) acetylacetonate $\text{Mn}(\text{acac})^3$ by mixing polymer

TABLE 1: Compositions of casting solution for the preparation of asymmetric PES/ $\text{Mn}(\text{acac})^3$ blend membranes.

Membrane	PES (wt%)	$\text{Mn}(\text{acac})^3$ (wt%)	$\text{Mn}(\text{acac})^3$ /acetonitrile (wt%)	NMP (wt%)
Bare PES	20	—	—	80
Blend PES/ $\text{Mn}(\text{acac})^3$	20	2	10	70

with a synthesized solution of $\text{Mn}(\text{acac})^3$ in acetonitrile will be investigated. The membranes were prepared by the wet phase inversion method. The membrane structure and properties will be subjected to full characterization techniques using SEM, AFM, mechanical testing system, and water contact angle measurements set-up. Desalination of seawater was applied as a final evaluating facility for the prepared blend membrane by RO-sea water desalination test.

2. Materials and Methods

2.1. Materials. Analytical grade N-methylpyrrolidone (NMP) as a solvent and Polyethersulfone (PES Ultrason E6020P with MW = 58,000 g/mol) were supplied by BASF Company (Germany). Technical grade acetylacetone was purchased from Fluka, and potassium permanganate (KMnO_4) was obtained from Sigma-Aldrich. Chemicals were used as received unless stated otherwise. All chemicals used in the experiments were of reagent grade. Real samples of the Mediterranean Sea were used in desalination experiments.

2.2. Fabrication of Asymmetric PES/ $\text{Mn}(\text{acac})^3$ Blend Membranes. The asymmetric PES/ $\text{Mn}(\text{acac})^3$ blend membranes were fabricated by phase inversion induced by an immersion precipitation method using casting solutions containing PES (20 wt%) and 10% solution of $\text{Mn}(\text{acac})^3$ dissolved in acetonitrile, and 70% N-methyl pyrrolidone (NMP) was used as solvent. The compositions of casting solutions for all membranes are depicted in Table 1.

$\text{Mn}(\text{acac})^3$ was synthesized by dissolving 5 g of KMnO_4 in 50 mL of distilled water with continuous stirring in batch system, after the dissolution was completed; the acetylacetone was added to the solution with continuous stirring. The formed dark shiny crystals of $\text{Mn}(\text{acac})^3$ were filtered off and dried in vacuum over fused CaCl_2 for 15 minutes [9].

The metalorganic solution was prepared by dispersing 2% of $\text{Mn}(\text{acac})^3$ in acetonitrile; then the mixture of casting solution was prepared by the addition of 10% of metalorganic solution to NMP solvent and the solution was stirred for 30 min; after that the PES was added gradually to the dope solution by continuous stirring for 4 h and the polymer mixture solution (casting solution) left in refrigerator for 24 h to remove air bubbles.

The prepared solution was casted onto a clean glass plate with 150 μm thickness. Subsequently, the glass plate was horizontally immersed in distilled water at room temperature. After primary phase separation and membrane solidification,

the membranes were stored in fresh distilled water for 24 h to guarantee the complete phase inversion. The membranes were dried by sandwiching them between two filter paper sheets for 24 h at room temperature [3–6].

2.3. Membrane Characterization

2.3.1. Scanning Electron Microscopy (SEM). Scanning electron microscopy (SEM) was used to observe the morphology of PES/Mn(acac)³ blend membrane, whereas the samples for cross-sectional view were coated with gold to provide electrical conductivity. The cross-sectional snapshots of membrane were taken with a JEOL 5410 scanning electron microscope (SEM) and conducted at 10 kV. Also, Mn(acac)³ crystals samples were grinded and coated with gold sputtering to provide electrical conductivity and the SEM micrographs were taken at 20 kV.

2.3.2. Mechanical Properties. Mechanical properties of PES and PES/Mn(acac)³ blend membranes were studied to determine the effect of metalorganic nanomaterials percentage on the membrane. The tensile strength and elongation of the membranes were measured using mechanical testing system (INSTRON-5500R). The gauge length and width of dumbbell tensile specimens were 6.2 and 0.16 mm, respectively. The specimens of membranes were placed between the grips of the testing machine and the tensile strength and elongation were calculated. The accuracy of the measurement is within $\pm 5\%$ [3].

2.3.3. Membrane Porosity and Contact Angle Measurements. Blend membranes PES/Mn(acac)³ porosity was measured by impregnating the membranes with water; after that the membrane was dried between two filter papers and weighted. After that, the wet membranes were placed in an air-circulating oven at 80°C for 24 h to be completely dry. Finally, the dry membranes were weighed and the porosity of membranes was calculated using the following equation [3]:

$$\varepsilon = \frac{W_0 - W_1}{V}, \quad (1)$$

where ε is the membrane porosity, W_0 and W_1 are the weights of wet and dry membranes in gram, respectively, and $V = A \cdot \delta$, where A is the membrane surface area in cm^2 and δ is the membrane thickness in cm. In order to minimize the experimental errors, the membrane porosity of each sample was measured several times (at least 3 times) and the average was calculated.

Distilled water was used for the contact angle (θ) measurement by the sessile drop method. The measurements were carried out four times for each membrane sample and the average values were calculated.

2.3.4. Atomic Force Microscopy (AFM). AFM topography images for bare PES and PES/Mn(acac)³ blend membrane were obtained using AFM, model Wet-SPM (Scanning Probe Microscope) Shimadzu made in Japan. The mean pores radius, surface area, and roughness were measured in scan

TABLE 2: Sea water sample analysis.

Parameters	Unit	Result
Total dissolved solids	mg/L	40,000
pH		7.5
Total hardness	mg/L	7000
Calcium hardness	mg/L	1800
Magnesium hardness	mg/L	5200
Sodium	mg/L	19,040
Alkalinity as bicarbonates	mg/L	14,000
Hydroxides	mg/L	0
Carbonates	mg/L	0

areas $2 \times 2 \mu\text{m}$. The contacting imaging mode in air was selected to study the membranes at room temperature. The membranes samples attached to steel disc with double sided adhesive tape. The standard deviation of various measurements was small, ranging from 0.9 Å on the smooth surfaces to 7.2 Å on the rough surfaces [25, 28].

2.4. Membrane Performance Measurements. The experiments were carried out on the laboratory desalination unit as shown in Figure 1. This system contains flat sheet membrane module of three openings for feeding, concentrate, and permeate. The feed was continuously fed to the membrane module from a closed feeding tank (5 liter) using a high pressure pump. The product was collected from downstream of the membrane module. The prepared PES/Mn(acac)³ blend and bare PES membranes were located in stainless steel plate module of 10 cm in diameter. In all experiments, sea water of concentration 40,000 ppm solution was continuously fed to the membrane module, at pressure 15 bars and temperature of 25°C. Table 2 illustrates the analysis of seawater sample.

For this system, the water flux J_w ($\text{Kg}/\text{m}^2 \text{h}$) is given by the following equation:

$$J_w = \frac{V \cdot \rho}{A \cdot t}, \quad (2)$$

where V is the volume of the pure water permeate (m^3), A is the effective area of the membrane (m^2), ρ is the water density (kg/m^3), and t is the permeation time (h).

The TDS of the produced water was measured using a conductivity meter called Adwa (AD 310), EC/temp meter made in Romania. It has an electrical conductivity range from 19.99 $\mu\text{S}/\text{cm}$ to 199.9 mS/cm , where 1 mS/cm equals approximately 670 ppm.

In addition, the salt rejection (SR%) was conducted in triplicate for each membrane and the average result was calculated using the following equation:

$$\text{SR}\% = \frac{C_f - C_p}{C_f} * 100, \quad (3)$$

where C_f and C_p are concentrations (mg/L) at feed bulk and permeate, respectively.

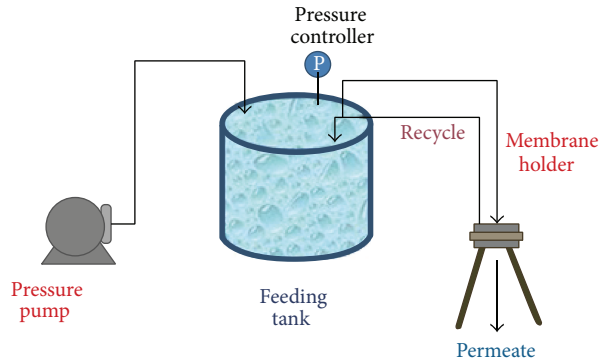


FIGURE 1: Schematic drawing of lab desalination testing unit.

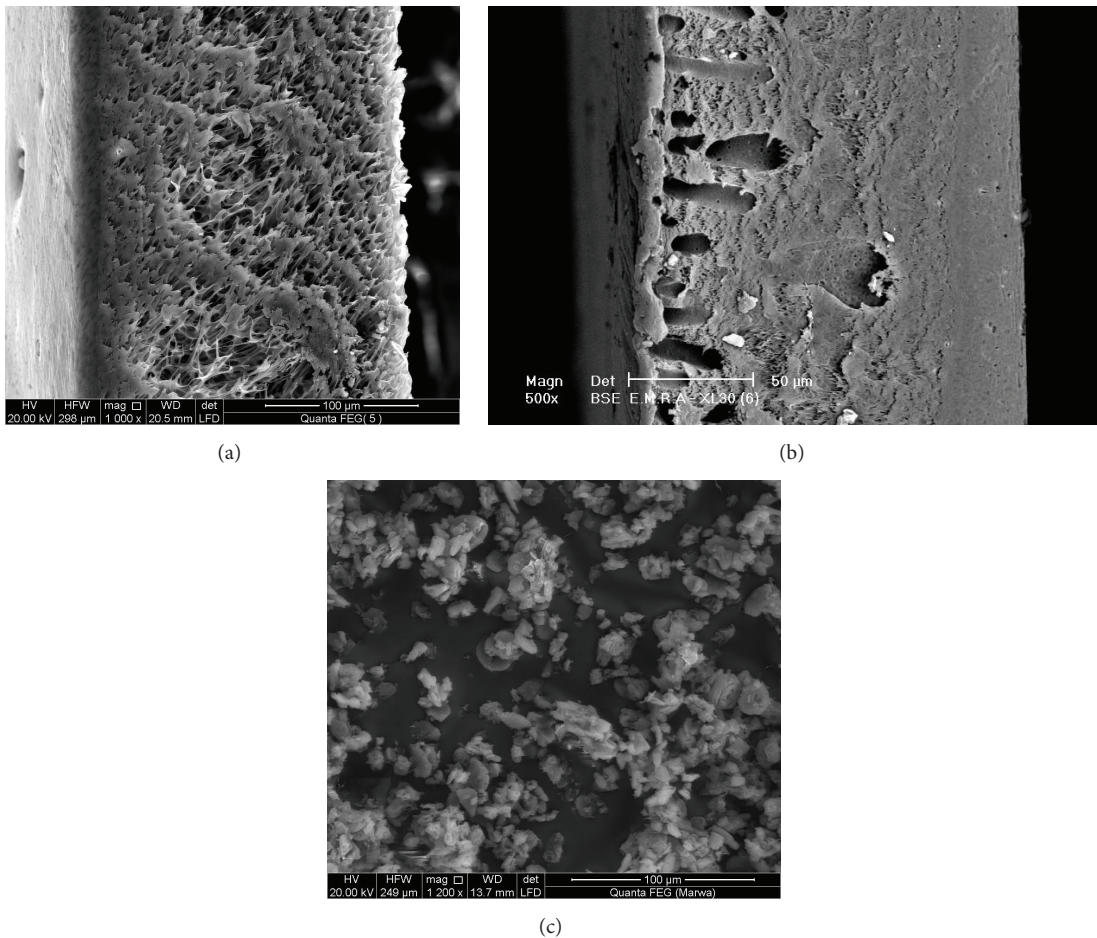


FIGURE 2: The cross-sectional SEM images of membranes: (a) bare PES and (b) blend membrane PES/Mn(acac)³; (c) is nano-Mn(acac)³ powder.

3. Results and Discussion

3.1. Membrane Characterization

3.1.1. *Scanning Electron Microscopy (SEM)*. Figure 2 shows cross-sectional SEM images of bare PES membrane and blended PES with Mn(acac)³. The blended membrane showed asymmetric membrane structure with a dense top

layer, a porous sublayer, and fully developed macrovoids at the bottom. Nevertheless, the formation of macrovoids was suppressed by the addition of Mn(acac)³ to the membrane structure as shown in Figure 2(b). Also, using Mn(acac)³ reduces the finger-like sublayer and increases the thickness of dense top layer.

These results might be explained by the fact that using Mn(acac)³ in the casting solution led to decrease in the

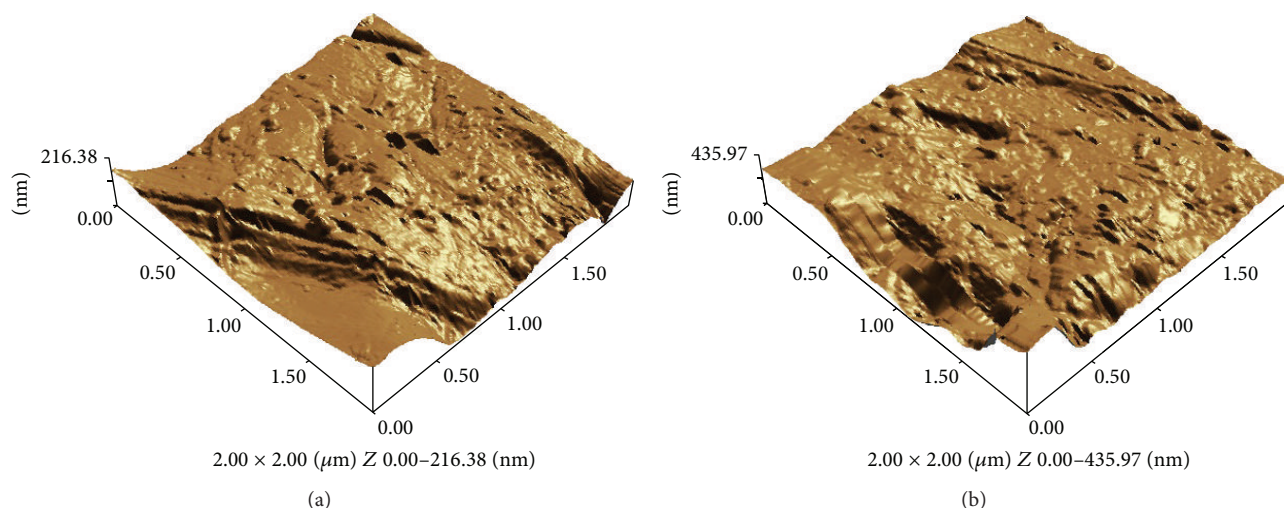


FIGURE 3: Three D-AFM images of (a) bare PES and (b) PES/Mn(acac)³ blend membrane.

membrane porosity, whereas the blank PES membrane in Figure 2(a) presents the porous spongy structure of the membrane.

Scanning electron micrographs were used for Mn(acac)³ nanocrystal surface view in the micrograph of Figure 2(c); the SEM image indicates that Mn(acac)³ powder was uniform fine particles with particle size of 146 nm and wall thickness 60 nm, which was measured in previous research of authors [9].

3.1.2. Mechanical Properties. The mechanical testing results indicate that the maximum tensile strength of bare PES was 40 kg/cm² and the maximum elongation was 4.5%, while the maximum tensile strength reached to 57.8 kg/cm² with elongation 6.2% for blend membrane PES/Mn(acac)³. Accordingly, using nanocrystals of metalorganic Mn(acac)³ in a membrane preparation led to improvement of the mechanical properties of the membrane, where blending between Polyethersulfone and Mn(acac)³ nanomaterials improves the mechanical properties by producing membranes able to withstand high pressures.

3.1.3. Membrane Porosity and Contact Angle. The overall porosity information of the prepared blend PES/Mn(acac)³ membrane and bare PES was presented in Table 3. The results of the porosity measurement revealed that the prepared PES/Mn(acac)³ blend membrane possessed a low porosity of 35% compared to 55% for bare PES membrane. The results indicate that using Mn(acac)³ as metalorganic compound in a membrane preparation can produce reverse osmosis membranes due to decrease in the membranes pores size.

Contact angle measurement of membranes is considered to be an important parameter for membrane characterization and indirect indication of the hydrophilicity and flux behavior. The contact angles were measured several times and then average values were reported. Table 3 illustrates the

TABLE 3: Membrane porosity and contact angle of bare PES and PES/Mn(acac)³ blend membrane.

Membrane type	Porosity (%)	Contact angle
Bare PES	55	80 ± 2°
PES/Mn(acac) ³ blend membrane	35	44 ± 2°

water contact angles of the blend membrane PES/Mn(acac)³ and bare PES. The bare PES membrane has higher contact angle (80 ± 2°), corresponding to the lower hydrophilicity. In the case of the blend membrane, lower contact angle was observed (44° ± 2) due to increase of the membrane hydrophilicity. So, it was anticipated that the blend membranes absorb more pure water into the membrane and therefore enhance the permeate flux rate.

3.1.4. Atomic Force Microscopy (AFM). Figures 3(a) and 3(b) present three-dimensional images AFM of bare PES and PES/Mn(acac)³ blend membrane. It can be observed that surface topography has difference for both bare PES and blend membrane. Mean pore sizes and pore size distribution of two different membranes were determined by AFM images as shown in Table 4. The table indicates that the mean pore size of bare PES is 0.076 ± 0.024 μm, which is larger than the mean pore size of PES/Mn(acac)³ blend membrane which is 0.003 ± 0.018 μm. According to that, the AFM images indicate that the pores size of PES/Mn(acac)³ blend membrane is close to the RO membrane pores size [1, 2]. AFM images indicate that the PES/Mn(acac)³ blend membrane is smoother than bare PES as shown in the image plane in Figure 4; this is due to excellent contrast to pores distribution, which can reduce surface roughness; likewise, blending of Polyethersulfone with Mn(acac)³ leads to chemical bonds between each other that makes homogeneity in the membrane surface compared to composite membranes, which are rough membranes due

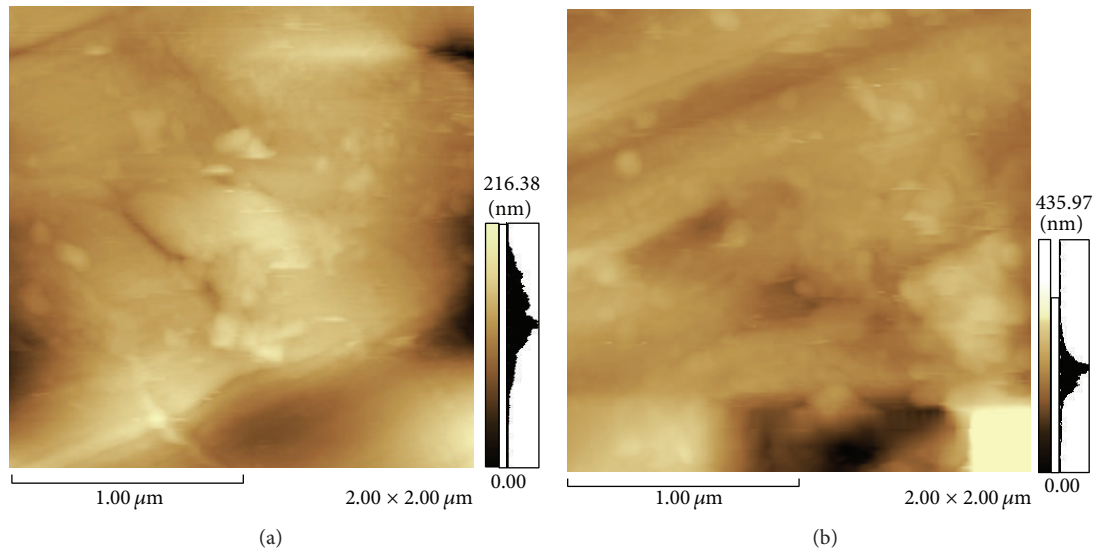


FIGURE 4: AFM plane images of (a) bare PES and (b) PES/Mn(acac)³ blend membrane.

TABLE 4: Parameters of surface morphology of PES/Mn(acac)³ blend membrane and bare PES were obtained from AFM images.

Membrane	Pores size, μm	Roughness, μm	Average mean height of peaks, μm
Bare PES	Mean pore size	2.4	216.38
	0.076 ± 0.024		
	Min. 0.003 Max. 0.35		
PES/Mn(acac) ³ blend membrane	Mean pore size	0.46	435.96
	0.003 ± 0.018		
	Min. 0.0002 Max. 0.017		

to precipitation of nanomaterials on the membrane surface [29]. The average roughness of the PES/Mn(acac)³ blend membrane is $0.46 \mu\text{m}$ compared to $2.4 \mu\text{m}$ for bare PES. Figure 5 illustrates the pores distribution on the membrane surface, where blending Mn(acac)³ with polymeric membrane materials (PES) reduces the membrane pores size and improves the pores distribution.

3.2. Membrane Performance Measurements. Average water permeation flux and average salt rejection % of PES/Mn(acac)³ blend membrane and bare PES were measured using the lab desalination unit on sea water solution of 40,000 ppm. The effects of using Mn(acac)³ on water flux and salt rejection % of prepared membranes are shown in Figures 6 and 7, respectively. The average flux of blend membrane reached $24.2 \text{ Kg/m}^2 \cdot \text{h}$, while the bare PES average flux reached $67.5 \text{ Kg/m}^2 \cdot \text{h}$. Figure 7 indicates that the average salt rejection of membranes increases to 99.5% with the addition of Mn(acac)³ in the casting solution to prepare blend membranes, while the average salt rejection was 20% using bare PES. Accordingly, the variations in hydrophilicity and

morphology of blend membrane and bare PES affect their performance. The bare PES has a higher permeate flux due to its higher porosity but it has lower salt rejection because it has no dense top layer. The blend membrane has a moderate permeate flux due to its hydrophilicity, while it has a higher salt rejection because it has a dense top layer with an increase in skin layer thickness. The metal acetylacetonate complex nanomaterials make cross-linking with polymeric membrane material and form the dense top layer of membrane [9, 13].

Table 5 illustrates a comparison of the performance of various kinds of membranes and the prepared membrane in this study based on salt rejection and permeate flux. This table indicates that the prepared PES/Mn(acac)³ blend membrane exhibits best membrane performance based on salt rejection and permeate at feed concentration of 40,000 ppm.

Polyethersulfone blended with carbon nanotubes (PES-CNT) provided highest permeate flux of $90 \text{ Kg/m}^2 \cdot \text{h}$ with 50% salt rejection of NaCl separation, compared with 99.5% salt rejection of new produced blend membrane PES/Mn(acac)³; the highest permeate flux of PES-CNT was related to the hexagonal geometric shape of carbon nanotubes, which could improve the pores distribution on the membrane surface [26]. The decrease in permeate flux to $24.2 \text{ Kg/m}^2 \cdot \text{h}$ using blend membrane PES/Mn(acac)³ was due to the high feed salt concentration, although it provided highest permeate flux compared to the PES/TFC membrane, PSf/PSAB blend membrane, and PS/Al metal membrane. These membranes also provided low salt rejection of different NaCl concentration solutions compared to the high salt rejection of producing blend membrane PES/Mn(acac)³.

4. Conclusion

- (i) The asymmetric PES/Mn(acac)³ blend membranes were successfully fabricated by the phase inversion method.

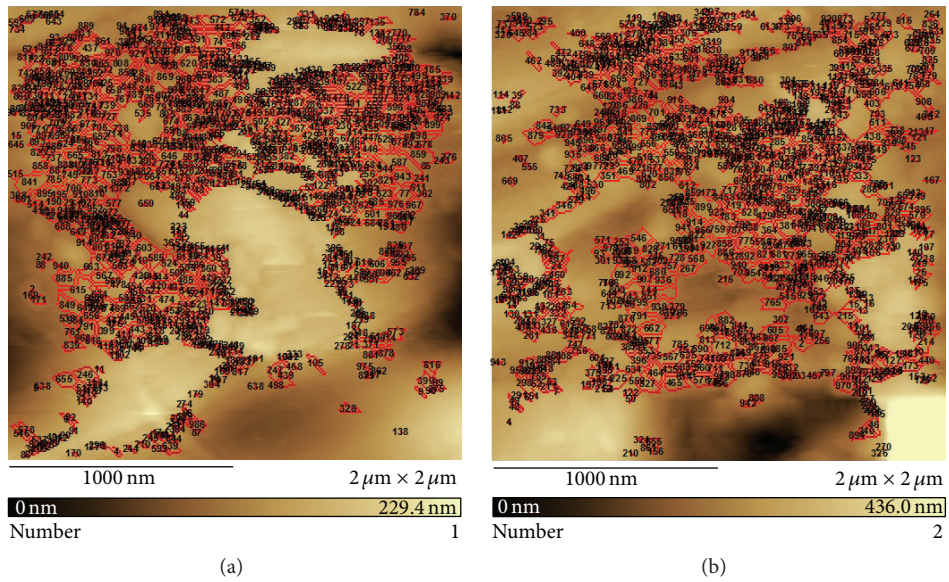


FIGURE 5: AFM pore distribution images of (1) bare PES and (2) PES/Mn(acac)³ blend membrane.

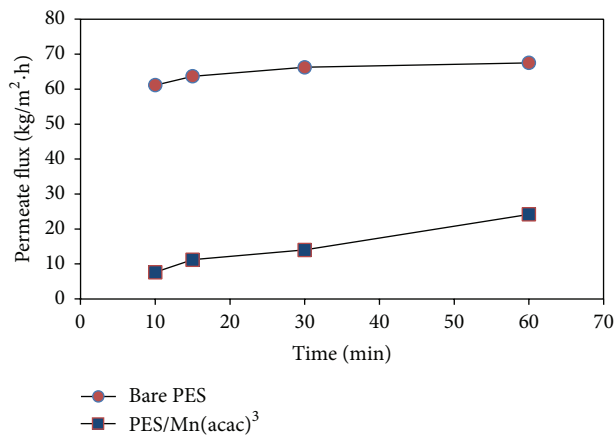


FIGURE 6: Average flux of PES/Mn(acac)³ blend membrane and bare PES.

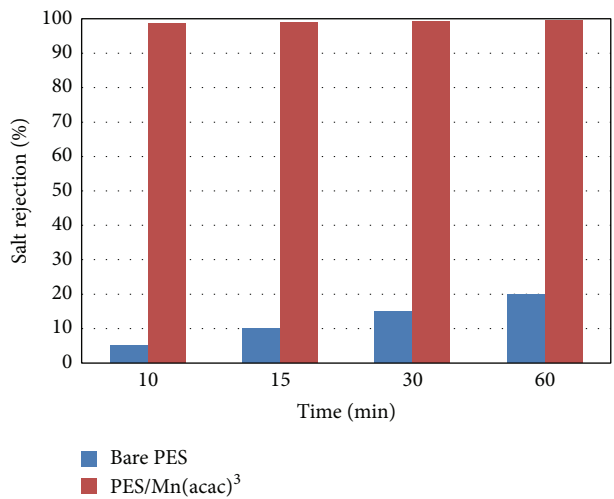


FIGURE 7: Average salt rejection % of PES/Mn(acac)³ blend membrane and bare PES.

TABLE 5: Comparison of the performance of different membranes.

Membrane*	Feed concentration. solution (ppm)	Salt rejection %	Permeate flux Kg/m ² .h	References
PES-CNT membrane	7000	50%	90	[26]
PES/TFC (TBAB) membrane	500	46%	21	[24]
PSf/PSAB membrane	1000	75%	19	[18]
PS/Al metal membrane	3500	42.22%	16.4	[27]
PES/Mn(acac) ³	40,000	99.5%	24.2	This work

*Where PES-CNT is Polyethersulfone blended with carbon nanotubes, PES/TFC (TBAB) membrane is thin film composite Polyethersulfone membrane and the surface is treated by tetrabutylammonium bromide (TBAB), PSf/PSAB is blended Polysulfone with polysulphonyl amino benzamide (PSAB), and PS/Al metal is composite membrane of vapor deposition of aluminum metal on Polysulfone membrane.

- (ii) The addition of Mn(acac)³ resulted in a decrease in the pores size, porosity, and low contact angle due to improvement in hydrophilicity compared with bare PES.
- (iii) The mechanical properties were improved after the addition of Mn(acac)³ in membrane preparation, where the tensile strength was 57.8 Kg/cm² with elongation being 6.2%.
- (iv) The blend membrane surface roughness is lower than bare PES due to the excellent contrast of pores distribution after addition of Mn(acac)³ nanoparticles. Also, blending the polymer (PES) with Mn(acac)³ leads to chemical bonds between each other making homogeneity in the membrane surface and smooth surface.
- (v) The salt rejection % of prepared blend membrane was improved, which was 99.5%; this means that Mn(acac)³ is good modifier for formation of RO Polyethersulfone membranes without further treatment of membrane surface.

Conflict of Interests

The authors confirm that there is no conflict of interests regarding the publication of this paper.

References

- [1] R. W. Baker, *Membrane Technology and Applications*, John Wiley & Sons, Chichester, UK, 2nd edition, 2004.
- [2] S. P. Nunes and K. V. Peinemann, *Membrane Technology in the Chemical Industry*, Wiley-VCH, Weinheim, Germany, 2001.
- [3] M. Shaban, H. AbdAllah, L. Said, H. S. Hamdy, and A. Abdel Khalek, "Titanium dioxide nanotubes embedded mixed matrix PES membranes characterization and membrane performance," *Chemical Engineering Research and Design*, vol. 95, pp. 307–316, 2015.
- [4] J. Kim and B. Van Der Bruggen, "The use of nanoparticles in polymeric and ceramic membrane structures: review of manufacturing procedures and performance improvement for water treatment," *Environmental Pollution*, vol. 158, no. 7, pp. 2335–2349, 2010.
- [5] M. Shaban, H. Hamdy, H. AbdAllah, L. Said, and A. Abdel Khalek, "Effects of TiO₂ NTs% on polyethersulfone/TiO₂ NTs membranes," *Journal of Materials Science and Engineering A*, vol. 5, no. 1-2, pp. 65–68, 2015.
- [6] J.-H. Li, Y.-Y. Xu, L.-P. Zhu, J.-H. Wang, and C.-H. Du, "Fabrication and characterization of a novel TiO₂ nanoparticle self-assembly membrane with improved fouling resistance," *Journal of Membrane Science*, vol. 326, no. 2, pp. 659–666, 2009.
- [7] X.-L. Wang, H.-J. Qian, L.-J. Chen, Z.-Y. Lu, and Z.-S. Li, "Dissipative particle dynamics simulation on the polymer membrane formation by immersion precipitation," *Journal of Membrane Science*, vol. 311, no. 1-2, pp. 251–258, 2008.
- [8] T.-H. Bae, I.-C. Kim, and T.-M. Tak, "Preparation and characterization of fouling-resistant TiO₂ self-assembled nanocomposite membranes," *Journal of Membrane Science*, vol. 275, no. 1-2, pp. 1–5, 2006.
- [9] M. S. Shalaby and H. Abdallah, "Preparation of manganese (III) acetylacetonate nanoparticles via an environmentally benign route," *Frontiers of Chemical Science and Engineering*, vol. 7, no. 3, pp. 329–337, 2013.
- [10] C. Pereira, S. Patrício, A. R. Silva et al., "Copper acetylacetonate anchored onto amine-functionalised clays," *Journal of Colloid and Interface Science*, vol. 316, no. 2, pp. 570–579, 2007.
- [11] C. Pereira, A. R. Silva, A. P. Carvalho, J. Pires, and C. Freire, "Vanadyl acetylacetonate anchored onto amine-functionalised clays and catalytic activity in the epoxidation of geraniol," *Journal of Molecular Catalysis A: Chemical*, vol. 283, no. 1-2, pp. 5–14, 2008.
- [12] S. Tangwiwat and S. J. Milne, "Barium titanate sols prepared by a diol-based sol-gel route," *Journal of Non-Crystalline Solids*, vol. 351, no. 12-13, pp. 976–980, 2005.
- [13] A. F. Shaaban, H. A.-E. Mostafa, M. A.-E. Khedr, and M. S. Mohamed, "Process engineering development for the manufacturing of manganese octoate on a pilot plant scale," *Chemical Engineering Research & Design*, vol. 90, no. 5, pp. 643–650, 2012.
- [14] S. Fujihara, "Sol-gel processing of fluoride and oxy fluoride materials," in *Handbook of Sol-Gel Science and Technology: Volume I—Sol-Gel Processing*, H. Kozuka, Ed., p. 219, Kluwer Academic Publishers, 2005.
- [15] J.-Y. Lee, C. Y. Tang, and F. Huo, "Fabrication of porous matrix membrane (PMM) using metal-organic framework as green template for water treatment," *Scientific Reports*, vol. 4, article 3740, 2014.
- [16] H. El Manakhly, N. Kenawy, A. M. Shaban, and M. M. Kamel, "Non agro-fiber material using as filter for industrial wastewater reclamation and reuse," *Egyptian Journal of Applied Sciences*, vol. 22, no. 10, pp. 290–300, 2007.
- [17] V. Vatanpour, S. S. Madaeni, A. R. Khataee, E. Salehi, S. Zinadini, and H. A. Monfared, "TiO₂ embedded mixed matrix

- PES nanocomposite membranes: influence of different sizes and types of nanoparticles on antifouling and performance," *Desalination*, vol. 292, pp. 19–29, 2012.
- [18] M. Padaki, A. M. Isloor, A. F. Ismail, and M. S. Abdullah, "Synthesis, characterization and desalination study of novel PSAB and mPSAB blend membranes with Polysulfone (PSf)," *Desalination*, vol. 295, pp. 35–42, 2012.
- [19] M. K. Chaudhuri, S. K. Dehury, S. S. Dhar, U. Bora, M. C. Choudary, and L. K. Mannepilli, US patent, 7282573 B2, 2007.
- [20] A. E. S. Sleightholme, A. A. Shinkle, Q. Liu, Y. Li, C. W. Monroe, and L. T. Thompson, "Non-aqueous manganese acetylacetonate electrolyte for redox flow batteries," *Journal of Power Sources*, vol. 196, no. 13, pp. 5742–5745, 2011.
- [21] A. A. Dakhel, "I–V Characteristics of tris(2,4-pentanedionato)manganese(III) thin films," *Journal of Non-Crystalline Solids*, vol. 351, no. 40–42, pp. 3204–3208, 2005.
- [22] M. Amirilargani, M. Sadrzadeh, and T. Mohammadi, "Synthesis and characterization of polyethersulfone membranes," *Journal of Polymer Research*, vol. 17, no. 3, pp. 363–377, 2010.
- [23] W. Haitao, Y. Liu, Z. Xuehui, Y. Tian, and D. Qiyun, "Improvement of hydrophilicity and blood compatibility on polyethersulfone membrane by blending sulfonated polyethersulfone," *Chinese Journal of Chemical Engineering*, vol. 17, no. 2, pp. 324–329, 2009.
- [24] J. Xiang, Z. Xie, M. Hoang, D. Ng, and K. Zhang, "Effect of ammonium salts on the properties of poly(piperazineamide) thin film composite nanofiltration membrane," *Journal of Membrane Science*, vol. 465, pp. 34–40, 2014.
- [25] N. Hilal, L. Al-Khatib, H. Al-Zoubi, and R. Nigmatullin, "Atomic force microscopy study of membranes modified by surface grafting of cationic polyelectrolyte," *Desalination*, vol. 184, no. 1–3, pp. 45–55, 2005.
- [26] E. Celik, H. Park, H. Choi, and H. Choi, "Carbon nanotube blended polyethersulfone membranes for fouling control in water treatment," *Water Research*, vol. 45, no. 1, pp. 274–282, 2011.
- [27] M. Padaki, A. M. Isloor, K. K. Nagaraja, H. S. Nagaraja, and M. Pattabi, "Conversion of microfiltration membrane into nanofiltration membrane by vapour phase deposition of aluminium for desalination application," *Desalination*, vol. 274, no. 1–3, pp. 177–181, 2011.
- [28] K. Boussu, B. van der Bruggen, A. Volodin, J. Snauwaert, C. van Haesendonck, and C. Vandecasteele, "Roughness and hydrophobicity studies of nanofiltration membranes using different modes of AFM," *Journal of Colloid and Interface Science*, vol. 286, no. 2, pp. 632–638, 2005.
- [29] K. C. Khulbe, C. Feng, and T. Matsuura, "The art of surface modification of synthetic polymeric membranes," *Journal of Applied Polymer Science*, vol. 115, no. 2, pp. 855–895, 2010.

